Influence of AlN buffer on electronic properties and dislocation microstructure of AlGaN/GaN grown by molecular beam epitaxy on SiC

B. S. Simpkins and E. T. Yu[a)]
Department of Electrical and Computer Engineering and Program in Materials Science and Engineering, University of California at San Diego, La Jolla, California 92093-0407

(Received 19 January 2003; accepted 1 March 2003; published 5 August 2003)

Electronic and structural properties of AlGaN/GaN heterostructures grown by molecular beam epitaxy on semi-insulating 4H–SiC substrates with and without an initial AlN nucleation layer are studied. Differences in microstructure were examined using scanning capacitance microscopy, which reveals negatively charged dislocations through capacitance variations, conductive atomic force microscopy, used to quantify the density of dislocation-related reverse-bias leakage paths, and x-ray diffraction (XRD). Samples grown without the AlN buffer exhibited features consistent with the commonly observed coalesced island structure, with negatively charged features, commonly associated with dislocations, occurring at the domain boundaries. Samples grown with an AlN buffer layer showed a more random distribution of negatively charged features, much broader symmetric XRD peak widths, and about 1 order of magnitude greater density of localized reverse-bias leakage paths. This difference in microstructure is expected to have significant influence on carrier mobilities and optical efficiencies, and may suggest improved nucleation schemes for device-quality nitride material. © *2003 American Vacuum Society.*
[DOI: 10.1116/1.1588647]

I. INTRODUCTION

Despite the large lattice mismatch (∼14%) and thermal expansion mismatch (nearly a factor of 3)[1] to GaN, sapphire remains the substrate of choice for GaN-based device fabrication due in large part to its relatively low cost. However, SiC offers an improved lattice (∼3.4%)[2] and thermal expansion match and provides greatly enhanced thermal conductivity needed for high-power device applications.[3,4] As with GaN growth on sapphire,[5] the early stages of nitride nucleation and growth on SiC dictate subsequent dislocation-related film properties as reflected in x-ray diffraction peak widths[6] and photoluminescence response.[7] The final dislocation microstructure plays a crucial role in optical[8] and electronic[9,10] device behavior and is therefore of critical interest.

In the current study, x-ray diffraction (XRD), conductive atomic force microscopy (C-AFM), and scanning capacitance microscopy (SCM) are used to examine the influence of an AlN buffer layer on the subsequent film microstructure including the densities and spatial distribution of negatively charged and highly conductive dislocation-related features.

II. EXPERIMENT

AlGaN/GaN heterojunction field effect transistor (HFET) structures were grown by molecular beam epitaxy (MBE) on semi-insulating on-axis 4H–SiC substrates. Active nitrogen species were supplied via an Applied Epi Unibulb rf plasma source. Before growth, substrates were cleaned sequentially with RCA2 (1:1:8 HCl:H2O2:H2O), de-ionized water, acetone, and methanol, then blown dry with N_2. The epitaxial layer structure consisted of a 25 nm $Al_{0.26}Ga_{0.74}N$ layer grown on a ∼3 μm GaN film at 750 °C under slightly metal-rich conditions. To determine the effects of a high-temperature (800 °C) AlN buffer layer on the properties of subsequently grown nitride layers, samples were grown under nominally identical conditions with and without a ∼60 nm AlN buffer layer deposited on the SiC substrate.

Symmetric x-ray diffraction rocking curves were recorded with a Phillips MRD4 x-ray diffractometer. C-AFM, which enables imaging of localized highly conductive leakage paths, was performed using a Digital Instruments MultiMode scanner modified to allow the application of an external bias and measurement of the resulting current. In the C-AFM measurement, a conductive probe tip (B doped diamond coated) is held in contact with and rastered over the sample while a dc bias (∼+10 V in our studies) is applied to the sample with the tip held at ground. Current through the probe tip is measured with a current amplifier that sends an output voltage signal, proportional to the current, through an auxiliary input to the control software. The resulting map reveals nonuniformities in sample conductivity. In particular, localized reverse-bias current leakage paths, which prior reports associate with pure screw dislocations, are imaged in nitride samples grown by MBE.[11,12]

Scanning capacitance microscopy was performed using a Digital Instruments Dimension 3100 SCM. In the SCM measurement, a W_2C-coated silicon probe tip is held in contact with and rastered over the sample while dc and ac biases are applied to the sample with respect to the grounded tip. The tip–sample capacitance is sensed using a transmission line resonant capacitance sensor,[13] which yields a measure of the slope of the capacitance–voltage curve, dC/dV, at the dc voltage value specified. Acquiring dC/dV response data over a range of applied dc biases allows the derivative of the

[a)]Electronic mail: ety@ece.ucsd.edu

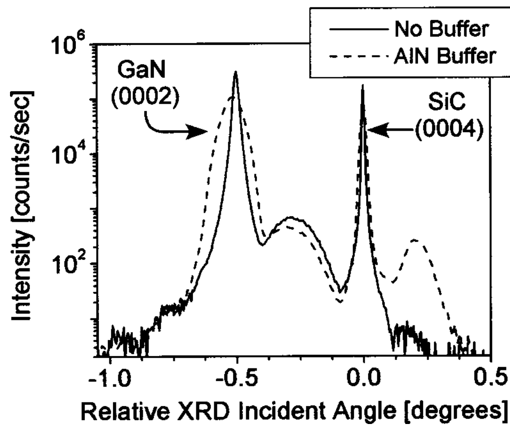

FIG. 1. Symmetric (0002) XRD scans for samples grown with and without an AlN buffer layer. The sample grown with the AlN buffer (dotted line) exhibits a larger peak width compared to the sample grown with no AlN layer (solid line). The FWHM of the peak are 341 and 138 arcsec.

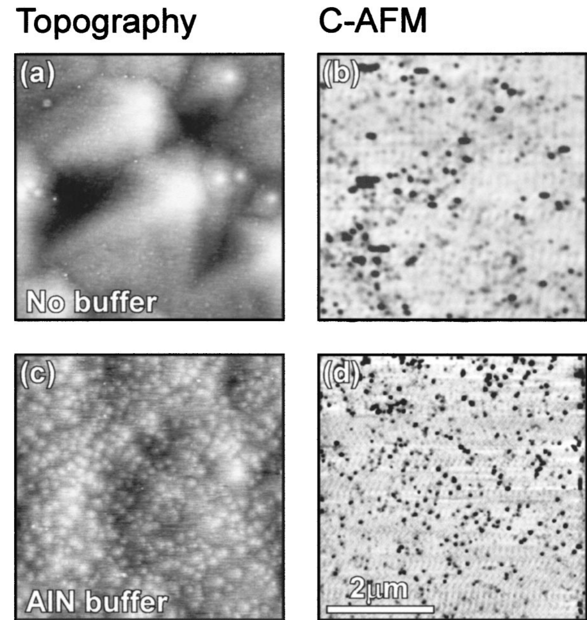

FIG. 2. C-AFM results showing topography and conductivity maps of representative 5×5 μm^2 areas. The sample grown without the AlN buffer exhibits: (a) smoother topography and (b) a reverse-bias leakage path density of $\sim10^8$ cm^{-2} while the sample utilizing the AlN buffer exhibits (c) rougher surface morphology and (d) $\sim10^9$ cm^{-2} reverse-bias leakage paths. Both topographic height scales are 7 nm and both current scales are 10 pA.

capacitance–voltage curve, and therefore the threshold voltage, to be extracted.[14] The spatial variation of this capacitance response reveals localized regions of decreased carrier density caused by the presence of negatively charged threading dislocations present in GaN.[15]

III. RESULTS AND DISCUSSION

Symmetric (0002) XRD curves for samples grown with and without an AlN buffer are shown in Fig. 1. Strain from dislocations having a Burger's vector with a component in the [0001] direction (screw and mixed dislocations) distorts the (0002) GaN plane spacing, causing a broadening of the symmetric diffraction peak.[16,17] As can be seen in Fig. 1, the GaN (0002) peak width for the sample grown with the AlN buffer layer is significantly broader than that for the sample grown without the buffer (341 and 138 arcsec, respectively). This is indicative of a lower concentration of screw-component dislocations[17] for the sample grown without the AlN buffer.

Figure 2 shows topographic and C-AFM images for representative 5×5 μm^2 areas of the samples grown without and with an AlN buffer layer. The topographic scans reveal a marked difference in surface morphology. As seen in Fig. 2(a), the sample grown without the AlN buffer exhibits a generally smoother topography compared to the sample grown with the AlN buffer [Fig. 2(c)], with rms roughness values of 1.8 and 3.6 nm, respectively, for a 10×10 μm^2 area. The dark regions in the reverse-bias current maps of Figs. 2(b) and 2(d) represent current leakage paths that have previously been found in GaN-based materials grown by MBE.[12] The density of leakage paths is $\sim10^8$ cm^{-2} for the sample with no AlN buffer [Fig. 2(b)] compared to $\sim10^9$ cm^{-2} for the sample grown with the AlN buffer layer [Fig. 2(d)]. Scanning probe data processing (i.e., constant or line by line background subtraction) may cause image artifacts; therefore, dark spots are counted as leakage paths only if they exhibit more than a 50 mV (5 pA) deviation from the mean value in the image. Previous work has associated these leakage features with pure screw dislocations[11] suggesting that, under our growth conditions, depositing the GaN film without an AlN buffer layer reduces the pure screw dislocation density by approximately 1 order of magnitude compared to films deposited on an AlN buffer. This hypothesis is also consistent with the previously discussed XRD results, which indicated a decrease in the screw-component dislocation density in the sample grown with no AlN buffer layer. The observed decrease in density of discrete leakage paths is expected to significantly influence the leakage current behavior of Schottky contacts subsequently fabricated on these materials.

The influence of the AlN buffer layer on the distribution of negatively charged dislocations was investigated using SCM. Negatively charged dislocations, occurring at columnar domain coalescence boundaries, cause a localized decrease in the two-dimensional electron gas (2DEG) carrier density and therefore a decrease in the threshold voltage.[14] These regions will experience depletion of the 2DEG at a smaller reverse-bias voltage than the neighboring regions of the sample which have higher 2DEG density. Spatial variations in this capacitance response for samples grown without and with the AlN buffer are shown in the SCM images of Figs. 3(a) and 3(b), respectively. These SCM images were acquired under dc bias conditions that cause regions of decreased carrier concentration in the 2DEG, likely near negatively charged dislocations,[14,15] to appear bright. Contrast in Fig. 3(a) suggests a microstructure, for the sample grown without the AlN buffer, composed of large domains (~2–5 μm diameter) with negatively charged dislocations (bright regions) at the boundaries between domains. This micro-

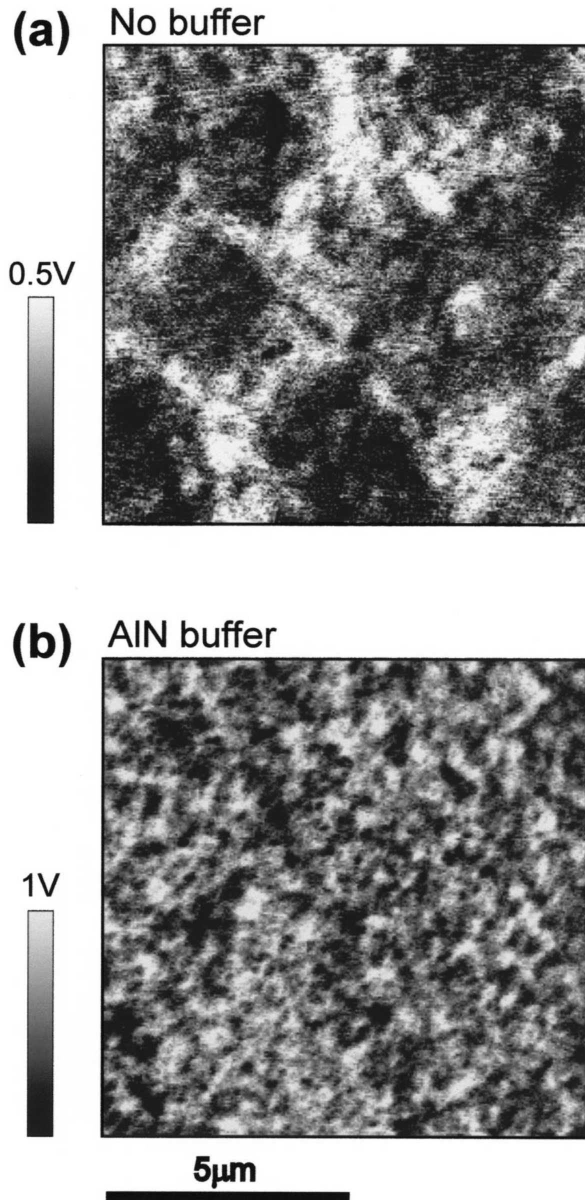

FIG. 3. SCM scans of representative $10\times10\ \mu m^2$ areas for samples grown (a) with no AlN buffer and (b) with the AlN buffer layer. Images were acquired with applied dc sample biases of (a) +5 V and (b) +3.5 V with a 1 V ac bias. Regions of decreased 2DEG density, associated with negatively charged dislocations, appear bright. Depositing GaN directly on SiC (a) results in a domain-dominated microstructure while growth on an AlN buffer (b) yields a seemingly random spatial distribution of negatively charged dislocations.

structure is commonly observed for GaN films grown under a variety of conditions,[15,18,19] although the characteristic domain size may vary. On the other hand, the sample grown with the AlN buffer, shown in Fig. 3(b), does not appear to exhibit the same domain-like microstructure. Contrast associated with negatively charged dislocations is clearly visible but their spatial distribution appears to be either random, or associated with domains whose radii are smaller than the characteristic diameter (~250 nm) of dislocation-induced SCM features seen in this work.

This change in film microstructure can be interpreted as a consequence of the nucleation behaviors of GaN and AlN on the SiC substrate. In the case of GaN nucleating directly on SiC (no AlN buffer), film growth occurs via island nucleation followed by island coalescence.[20] This results in the domain structure observed in this experiment and in many other investigations.[5,15,19,21] The sample employing the AlN buffer layer undergoes a fundamentally different nucleation process. On the basis of detailed XRD strain analysis applied to MBE GaN films grown with AlN and GaN buffer layers on SiC,[20] it has been suggested that the AlN buffer layer grows pseudomorphically on the SiC substrate due its smaller lattice mismatch (~1%). If the AlN buffer layer does form pseudomorphically and the subsequent GaN film nucleates and grows in a two-dimensional mode, a domain structure, with dislocations forming at coalescence boundaries, would not be expected. Misfit dislocations would likely occur at the GaN/AlN interface and could be formed by the nucleation of dislocation loops at step edges at the film surface followed by glide toward and across the interface.[22] This creates two threading dislocations for each misfit segment formed (one thread at each end of the misfit segment, thus creating a half loop).

However, pseudomorphic nucleation, along with the accompanying dislocation arrangement, may not be beneficial for device performance. Researchers using organometallic vapor phase epitaxy to deposit GaN on a high temperature AlN nucleation layer on SiC also found a domain-free, single crystal microstructure,[23] however, high dislocation densities ($\sim10^9\ cm^{-2}$) were still present. If negatively charged dislocations were randomly distributed, their carrier scattering[9] and nonradiative recombination effects[24] could be more pronounced than if the same density of these centers were clustered at coalescence boundaries. The degradation effects of dislocations are expected to influence only carriers within a diffusion length of the defect. If the negatively charged dislocations were located preferentially at coalescence boundaries, large areas of the sample would be essentially free of such dislocations. Indeed, sheet resistance behavior exhibits this behavior, with values of 540 and 340 Ω/□, measured for samples with and without an AlN buffer, respectively. Additionally, we have shown here that the density of localized reverse-bias leakage paths is approximately an order of magnitude higher for the film grown on an AlN buffer layer. These leakage paths can be the primary cause of reverse-bias leakage current in MBE-grown GaN-based devices,[25] and it is therefore expected that devices fabricated on films utilizing an AlN buffer on SiC will suffer from increased leakage current when compared to the GaN films grown directly on SiC in our study.

IV. CONCLUSION

We have characterized differences in film microstructure and in electronic properties for AlGaN/GaN HFET structures grown with and without an AlN buffer layer on semi-insulating 4H–SiC (0001). Films grown without the AlN buffer layer exhibited narrower (0002) symmetric XRD peak widths, indicating a decreased density of screw-component

dislocations. C-AFM measurements revealed a 1 order of magnitude fewer reverse-bias leakage paths, occurring at pure screw dislocations, for the sample with no AlN buffer layer. Negatively charged features, commonly associated with dislocations and imaged by SCM, were shown to be spatially distributed in a configuration consistent with dislocation formation at boundaries between coalesced islands for the sample with no AlN buffer, while appearing to be randomly distributed for the sample grown with an AlN buffer. This can be explained as a consequence of the pseudomorphic growth of AlN on SiC, which is in contrast to the more commonly observed island nucleation and coalescence mechanisms observed for most nitride films.

ACKNOWLEDGMENTS

Part of this work was supported by the Raytheon Corporation through the Raytheon University DR program, and by the National Science Foundation (Award No. DMR 0072912).

[1] T. Sasaki and S. Zembutsu, J. Appl. Phys. **61**, 2533 (1987).
[2] S. C. Jain, M. Willander, J. Narayan, and R. Van Overstraeten, J. Appl. Phys. **87**, 965 (2000).
[3] S. T. Sheppard, K. Doverspike, W. L. Pribble, S. T. Allen, J. W. Palmour, L. T. Kehias, and T. J. Jenkins, IEEE Electron Device Lett. **20**, 161 (1999).
[4] O. Aktas, Z. F. Fan, A. Botchkarev, S. N. Mohammad, M. Roth, T. Jenkins, L. Kehias, and H. Morkoc, IEEE Electron Device Lett. **18**, 293 (1997).
[5] X. H. Wu, P. Fini, E. J. Tarsa, B. Heying, S. Keller, U. K. Mishra, S. P. Denbaars, and J. S. Speck, J. Cryst. Growth **189/190**, 231 (1998).
[6] V. Ramachandran, R. M. Feenstra, W. L. Saney, L. Salamanca-Riba, and D. W. Greve, J. Vac. Sci. Technol. A **18**, 1915 (2000).
[7] R. Lantier, A. Rizzi, D. Guggi, H. Lüth, B. Neubauer, D. Gerthsen, S. Frabboni, C. Coli, and R. Cingolani, MRS Internet J. Nitride Semicond. Res. **4S1**, G3.50 (1999).
[8] F. A. Ponce, D. P. Bour, W. Götz, and P. J. Wright, Appl. Phys. Lett. **68**, 57 (1996).
[9] H. M. Ng, D. Doppalapudi, T. D. Moustakas, N. G. Weimann, and L. F. Eastman, Appl. Phys. Lett. **73**, 821 (1998).
[10] D. Jena, A. C. Gossard, and U. K. Mishra, Appl. Phys. Lett. **76**, 13 (2000).
[11] J. W. Hsu, M. J. Manfra, R. J. Molnar, B. Heying, and J. S. Speck, Appl. Phys. Lett. **81**, 79 (2002).
[12] E. J. Miller, D. M. Schaadt, E. T. Yu, C. Poblenz, C. Elsass, and J. S. Speck, J. Appl. Phys. **91**, 9821 (2002).
[13] R. C. Palmer, E. J. Denlinger, and H. Kawamoto, RCA Rev. **43**, 194 (1982).
[14] D. M. Schaadt, E. J. Miller, E. T. Yu, and J. M. Redwing, J. Vac. Sci. Technol. B **19**, 1671 (2001).
[15] P. J. Hansen *et al.*, Appl. Phys. Lett. **72**, 2247 (1998).
[16] B. D. Cullity, *Elements of X-Ray Diffraction*, 2nd ed. (Addison-Wesley, Menlo Park, CA, 1978), pp. 285–292.
[17] B. Heying, X. H. Wu, S. Keller, Y. Li, D. Kapolnek, S. P. Denbaars, and J. S. Speck, Appl. Phys. Lett. **68**, 643 (1996).
[18] T. Metzger *et al.*, Philos. Mag. A **77**, 1013 (1998).
[19] V. Potin, P. Ruterana, G. Nouet, R. C. Pond, and H. Morkoc, Phys. Rev. B **61**, 5587 (2000).
[20] P. Waltereit, O. Brandt, A. Trampert, M. Ramsteiner, M. Reiche, M. Qi, and K. H. Ploog, Appl. Phys. Lett. **74**, 3660 (1999).
[21] J. Lu, L. Haworth, D. I. Westwood, and J. E. Macdonald, Appl. Phys. Lett. **78**, 1080 (2001).
[22] S. Mahajan, Mater. Res. Soc. Symp. Proc. **410**, 3 (1996).
[23] T. W. Weeks, Jr., M. D. Bremser, K. S. Ailey, E. Carlson, W. G. Perry, and R. F. Davis, Appl. Phys. Lett. **67**, 401 (1995).
[24] T. Sugahara, H. Sato, M. Hao, Y. Naoi, S. Tottori, K. Yamashita, K. Nishino, L. T. Romano, and S. Sakai, Jpn. J. Appl. Phys., Part 2 **37**, L398 (1998).
[25] E. J. Miller, D. M. Schaadt, E. T. Yu, P. Waltereit, C. Poblenz, and J. S. Speck, Appl. Phys. Lett. **82**, 1293 (2003).